

## Reconstruction of the Radial Distribution Function from EXAFS: New Trends and Comparative Analysis of Different Methods

A. Kuzmin

*Institute of Solid State Physics, 8 Kengaraga str., 1063 Riga, Latvia*

**Abstract.** In spite of the EXAFS contribution from the first shell, where multiple-scattering effects are absent in most cases, is described by the simple formalism, the development and improvement of practical procedures for the extraction of reliable structural information are still topical. In present work, the possibilities and limitations of several different methods such as model based technique [1], cumulant approach [2], splice technique [6] and recently developed model-independent method for radial distribution function determination [4,5] are discussed. A comparative analysis of the methods is presented on an example of their applications to a number of model distributions and to real crystalline and disordered systems.

Great advantage of the x-ray absorption spectroscopy (XAS) compared to diffraction techniques is its short range order and site selective sensitivity that makes XAS a unique probe of static distortions and anharmonic vibrational effects within the first coordination shell around absorber. However, in spite of the EXAFS contribution from the first shell can be described in most cases within simple curved-wave single-scattering formalism, there is still no certain analysis procedure which allows to extract reliable structural information on the first-shell radial distribution function (RDF) in an arbitrary system.

At present time, there are several approaches which are commonly used on practice for the 1st-shell EXAFS analysis: (i) model-dependent techniques, based on the parametrized RDF [1] or the cumulant approach [2]; (ii) model-independent methods for the *ab initio* RDF reconstruction as regularization technique [3]; "freestyle" [4] and "constrained" [5] methods; (iii) splice technique [6]. The splice method [6] is in a separate group because in spite of it is related to the direct inversion procedure, it uses the finite cumulant expansion for the reconstruction of the low-k EXAFS signal. These three approaches can be summarised within the framework of the general scheme (Figure 1) which shows different ways to the determination of the RDF  $G(R)$  from the 1st-shell EXAFS signal  $\chi(k)$ , singled out from the total experimental signal by the back-Fourier transform. Each of the described approaches has its strong and weak sides which we are going to discuss further.

In the splice approach, the accuracy of the RDF determination is limited by the following two main factors: (a) the validity of the cumulant expansion for the reconstruction of the EXAFS signal in the range  $0 < k < k_{\min}$  and (b) the value of the EXAFS signal at  $k = k_{\max}$ : if  $|\chi(k_{\max})| > 0$  then the Fourier integration is performed over the EXAFS signal  $\chi(k)$  abruptly cutted at  $k_{\max}$  that results in the distortion of the calculated RDF shape due to appearance of the additional harmonics. The last effect is demonstrated in Figure 2 on the example of the model distribution composed of two Gaussian peaks ( $N_1 = 2$ ,  $R_1 = 1.8 \text{ \AA}$ ,  $\sigma_1 = 0.05 \text{ \AA}$ ,  $N_2 = 1$ ,  $R_2 = 2.1 \text{ \AA}$ ,  $\sigma_2 = 0.06 \text{ \AA}$ ). Here the simulated EXAFS signal is used in the k-range from  $k_{\min} = 0$  to  $k_{\max}$  so that no splicing is necessary however the shape of the obtained RDF's (dashed lines) show strong dependence on  $k_{\max}$  leading to large disagreement between initial and final RDF's when  $k_{\max} < 12$ . Note that the influence of the  $k_{\max}$  reduction is much smaller for the approach described in [5]: here the decrease of  $k_{\max}$  leads mainly to the broadening of the RDF (solid lines in Figure 2) that is related to the expected lowering of the resolution  $\Delta R \approx \pi/2k_{\max}$ .

The model-dependent techniques, among which the Gaussian approximation is the most widely used [1], allows to reduce significantly a number of fitting parameters and a correlation between them. However, if the true shape of the distribution differs from the model RDF then errors in the position, intensity and width of peaks appear in the obtained RDF. This conclusion is illustrated by the results of model calculations presented in Figure 3. Here the model RDF were chosen to cover different RDF shapes having a degree of distortion and an asymmetry frequently occurring in real situations. The 1st RDF (in (a)) corresponds to the simplest case of one Gaussian ( $N = 1$ ,  $R = 1.8 \text{ \AA}$ ,  $\sigma = 0.06 \text{ \AA}$ ). The 2nd RDF (in (b)) consists of two slightly separated Gaussians ( $N_1 = 2$ ,  $R_1 = 1.8 \text{ \AA}$ ,  $N_2 = 1$ ,  $R_2 = 1.9 \text{ \AA}$ ,  $\sigma_1 = \sigma_2 = 0.06 \text{ \AA}$ ). The 3rd RDF (in (c)) is the same as in Figure 2. The 4th RDF (in (d)) represents the case of strongly asymmetric non-Gaussian distribution with a long tail observed in superionic materials. The agreement between the model and calculated RDF's is estimated by  $\epsilon = 100\% \cdot \sum(G_{\text{calc}} - G_{\text{model}})^2 / \sum(G_{\text{model}})^2$ . As one can see, the Gaussian approximation fails in the case (d), and the cumulant approach in the case (c), while the model-independent approach [5] is able to describe more or less well any type of the RDF. The application of the method [5] to real crystalline and amorphous systems can be found in [7] where its comparison with some conventional techniques such as Gaussian multi-shell approximation and splice technique is also presented.

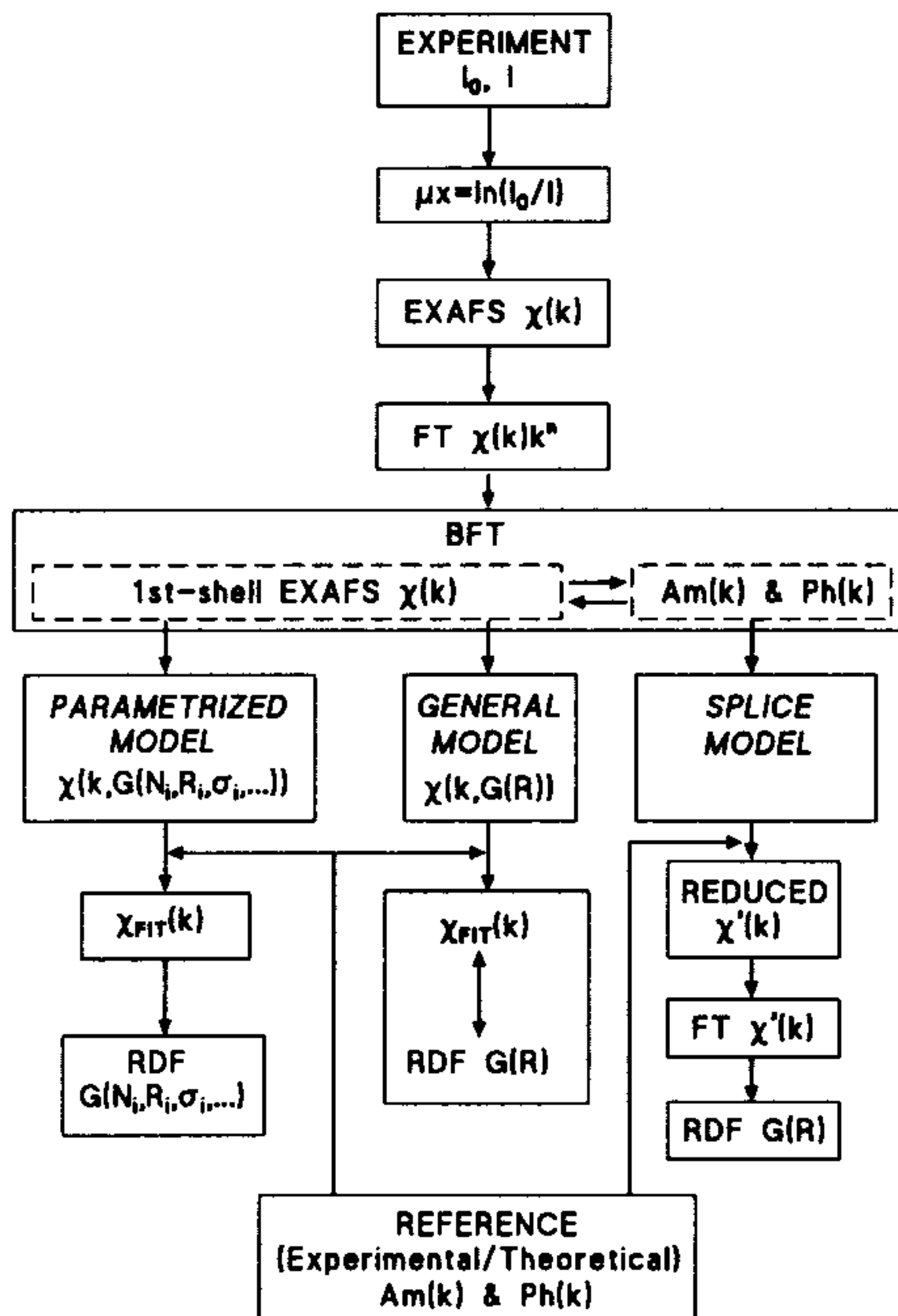


Figure 1: General scheme of the first-shell EXAFS analysis.

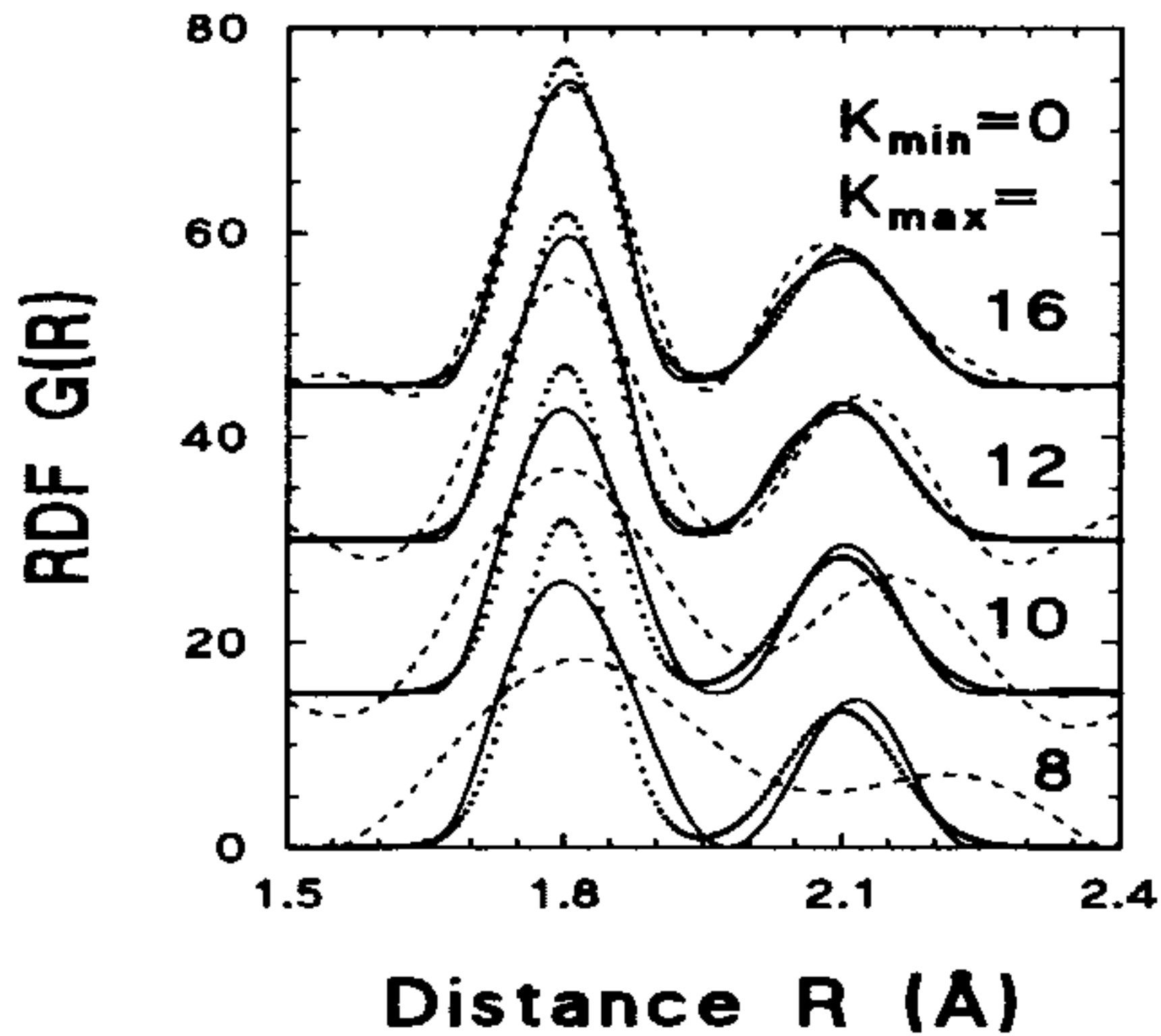


Figure 2: Influence of  $k_{max}$  on the shape of the RDF's obtained by splice technique [6] (dashed lines) and model-independent method [5] (solid lines). Model RDF is shown by dotted line.

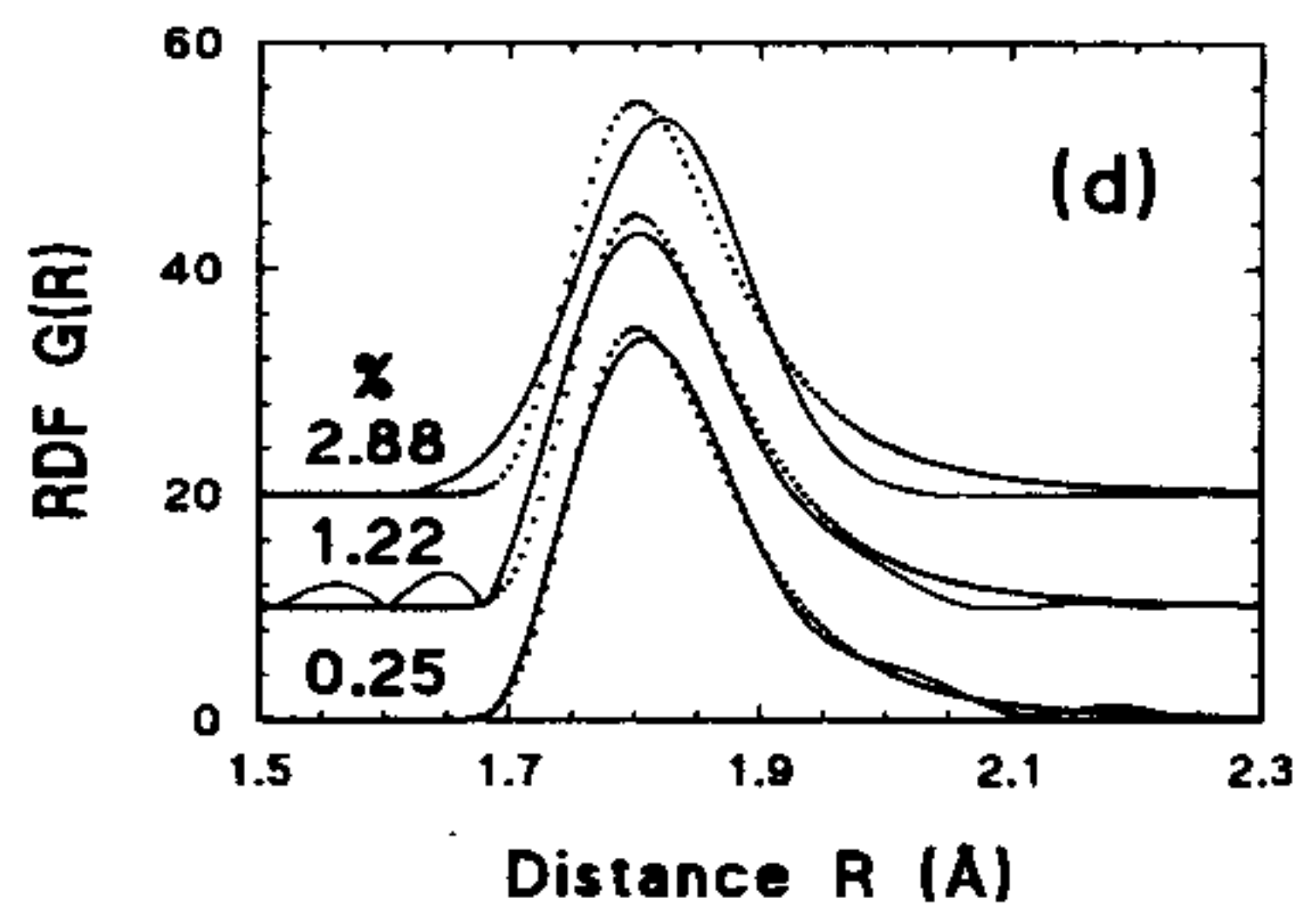
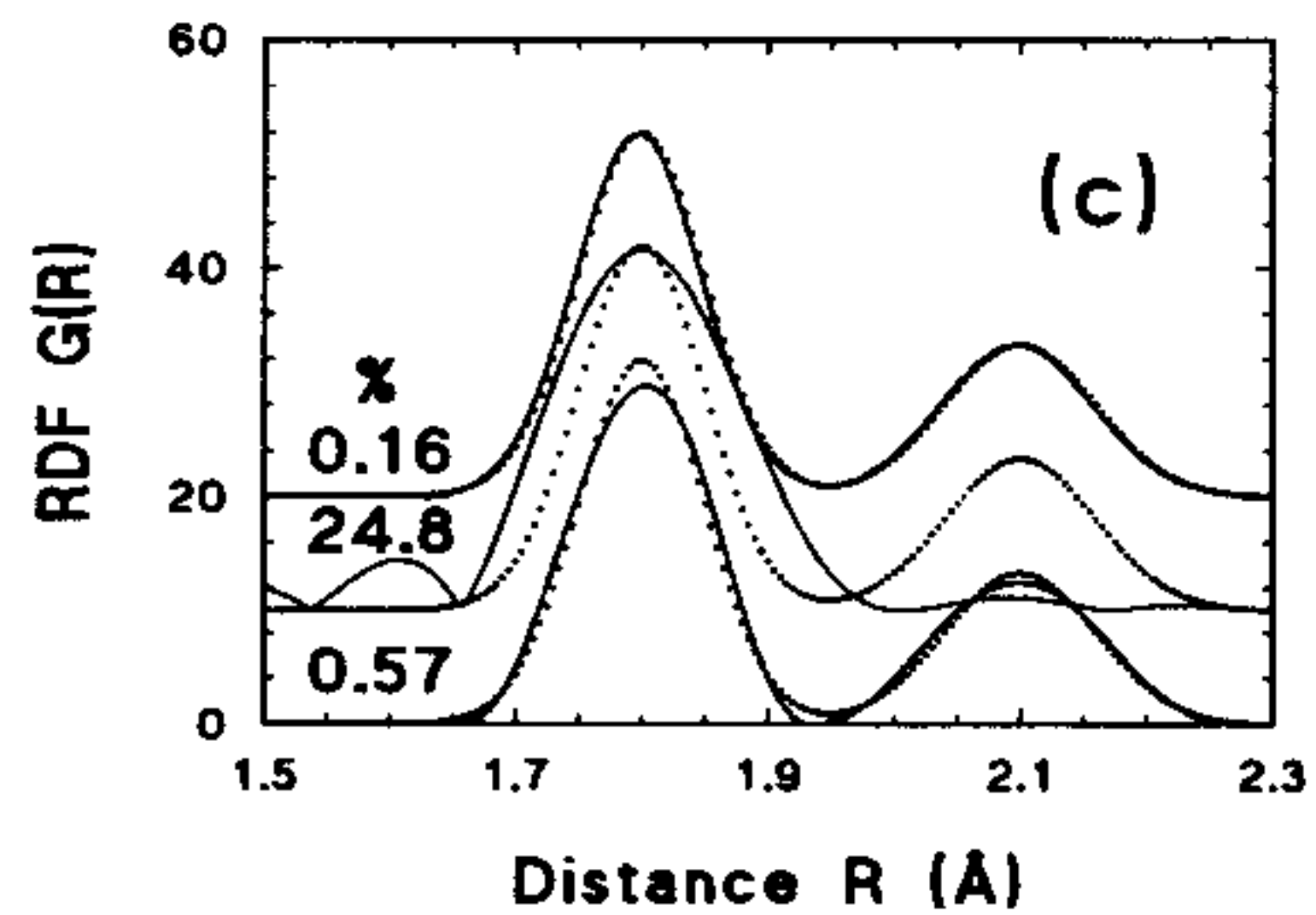
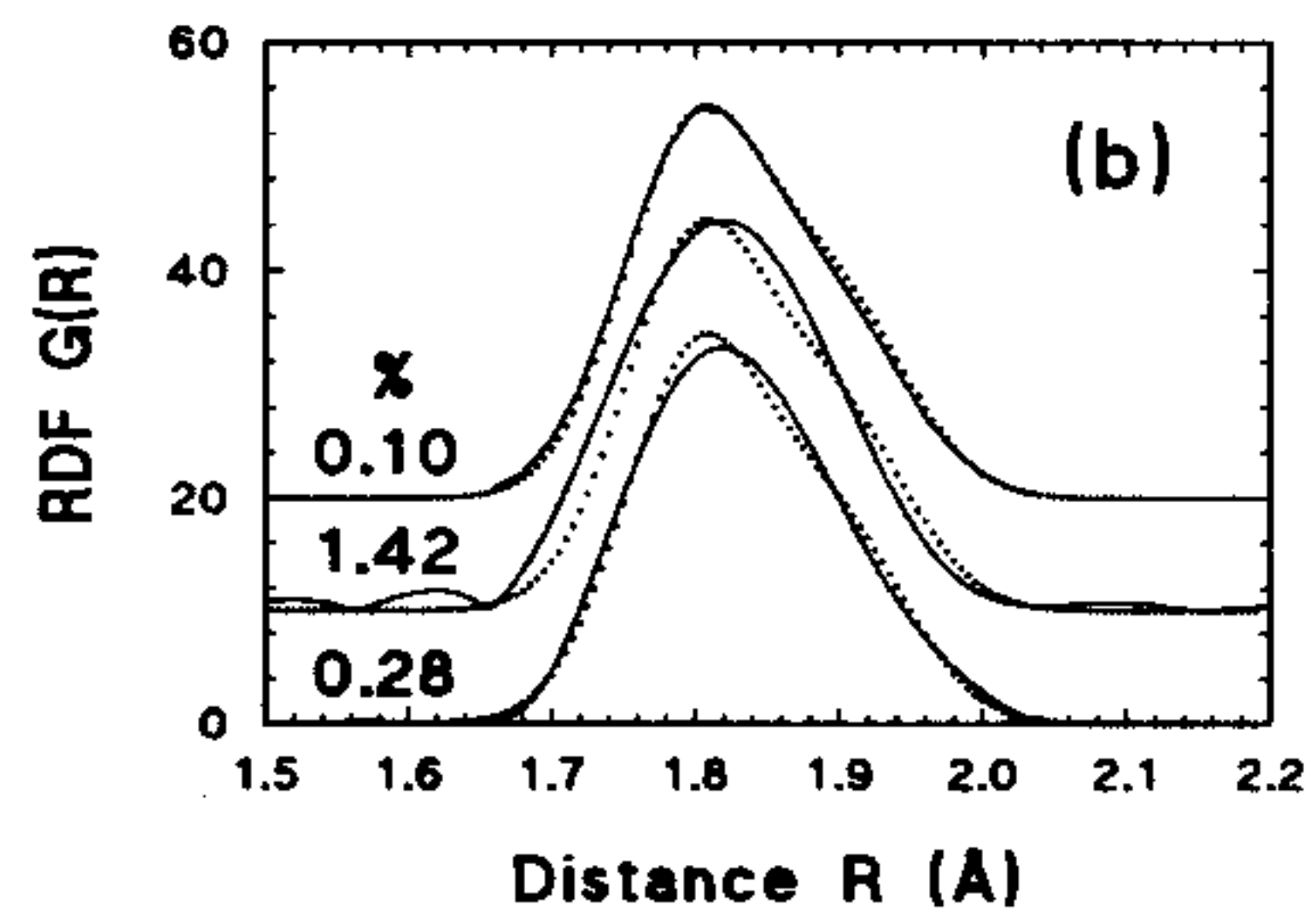
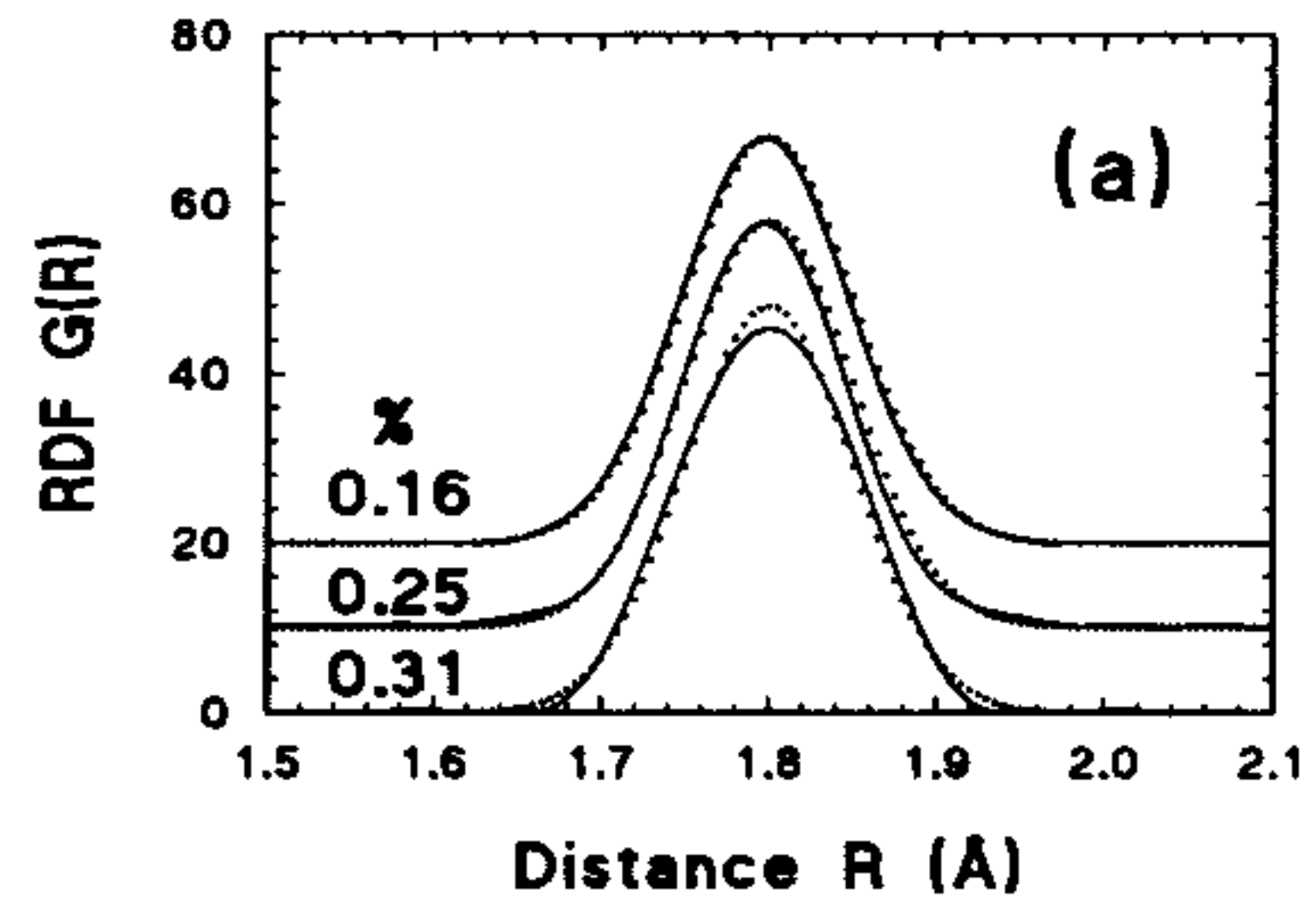


Figure 3: Comparison of the Gaussian [1] (upper solid curves), cumulant [2] (middle solid curves) and model-independent [5] (lower solid curves) methods. Dotted lines are model RDF's. The values of  $\epsilon$  (in %) are shown for each RDF.

## References

- [1] Stern E.A., *Phys. Rev. B* **10** (1974) 3027-3037; Filipponi A. and Di Cicco A., *Phys. Rev. B* **51** (1995) 12322-12336.
- [2] Bunker G., *Nuclear Instrum. Methods* **207** (1983) 437-444.
- [3] Babanov Yu.A., Vasin V.V., Ageev A.L. and Ershov N.V., *Phys. Status Solidi b* **105** (1981) 747-754.
- [4] Kizler P., "Freestyle EXAFS fit algorithm for systems with large disorder", Proc. 6th Inter. Conf. on X-ray Absorption Fine Structure, York 5-11 August 1990, S.S. Hasnain Ed. (Ellis Horwood, Singapore, 1991) pp.78-80.
- [5] Kuzmin A., *Physica B* **208&209** (1995) 175-176; Kuzmin A., (to be published).
- [6] Stern E.A., Ma Y., Hanske-Petitpierre O. and Bouldin C.E., *Phys. Rev. B* **46** (1992) 687-694.
- [7] Kuzmin A. and Purans J., *J.Phys. IV France* (contribution to this Proceedings); Kuzmin A., Purans J., Parent Ph. and Dexpert H., *J.Phys. IV France* (contribution to this Proceedings); Kuzmin A., Purans J., Dalba G., Fornasini P. and Rocca F., *J.Phys. IV France* (contribution to this Proceedings).